Surface Science 612 (2013) 82–89

Contents lists available at SciVerse ScienceDirect

Surface Science

journal homepage: www.elsevier.com/locate/susc

Copper(110) surface in thermodynamic equilibrium with water vapor studied from first principles

Amirreza Baghbanpourasl [a,*], Kurt Hingerl [a], Stefan Wippermann [b], Wolf Gero Schmidt [b]

[a] Center for Surface and Nanoanalytics, Johannes Kepler University Linz, Altenbergerstr. 69, A-4040 Linz, Austria
[b] Lehrstuhl für Theoretische Physik, Universität Paderborn, 33095 Paderborn, Germany

ARTICLE INFO

Article history:
Received 9 November 2012
Accepted 24 February 2013
Available online 1 March 2013

Keywords:
Copper
Water
Adsorption
DFT
Cu(110)
Phase diagram

ABSTRACT

The adsorption of water monomers, small water clusters, water chains and water thin films on the Cu(110) surface is studied by density-functional theory (DFT) as well as using a semi-empirical scheme to include dispersion forces (DFT-D). Among the cluster structures, tetramers are most favorable. The calculated surface phase diagrams show that out of the multitude of Cu(110)-adsorbed water structures studied here (and proposed in earlier experimental and theoretical works) only monolayers resembling water ice, water-hydroxyl group layers stabilized by Bjerrum defects, and – in a narrow range of the water chemical potential – chains assembled from water pentagons are thermodynamically stable. The inclusion of van der Waals interaction increases the calculated adsorption energies, but has only minor consequences for the energetic ordering of adsorption geometries. It increases the calculated desorption temperatures from 60 K in low pressures until 150 K in near ambient pressures.

© 2013 Elsevier B.V. All rights reserved.

1. Introduction

The interaction of water with solid surfaces is fundamental to research in fields as diverse as corrosion, cellular biology, and atmospheric chemistry [1,2]. Despite substantial research efforts, the structural properties of water are at best incompletely understood. This holds for the ubiquitous liquid phase [3,4] as well as for thin substrate-supported water films and clusters prepared in the laboratory [5–7]. In order to explore the mutual interaction of water monomers and its modification by the substrate, the experimental and theoretical research focuses on well defined model systems that are accessible to both advanced surface-sensitive probes as well as *first-principles* calculations. The adsorption of water on the Cu(110) surface is one prominent example in this respect. However, while many experimental and theoretical studies have been devoted to this system, the results do not yield a consistent picture yet.

An early experimental study by Spitzer and Lüth [8] indicates molecular adsorption for temperatures below 90 K, with the H_2O molecules bonded at the oxygen. They observed dissociative adsorption of water, occurring at temperatures above 90 K. Preference for an island growth of weakly bonded water monomers with local c(2 × 2) has been concluded by Mariani and Horn [9] from photoemission experiments. The experimental finding of dissociative adsorption at relatively low temperatures [8,10] was attributed to radiation damage in Ref. [11]. Even up to 428 K surprisingly large quantities of molecular water were detected [12]. Using low-energy electron diffraction, Schiros et al. [13] found a hydrogen-bonded, hexagonal (7 × 8) structure for the molecularly adsorbed water monolayer. Yamamoto et al. [14] ascribed the wettability of Cu(110) to partial dissociation of water molecules on this surface. An autocatalytic water dissociation on Cu(110) at near ambient conditions is reported in Ref. [15]. In some cases, stoichiometry deviations in the water overlayer result from adsorption on O-preadsorbed substrates or electron bombardment [14,16]. Scanning tunneling microscopy (STM) experiments [16] gave microscopic insight in the partially H_2O dissociated structure and indicated its stabilization by Bjerrum defects, possibly mediating multilayer growth. Also, a plethora of further water structures on Cu(110) were observed by STM, indicating the formation of chains consisting of H_2O and OH [17] or assembled from ring-like structures [18]. These rings were attributed to water pentagons [19], thus contrasting with the ubiquitous hexagon structures resembling ice Ih typically found for metal-adsorbed water.

The experimental studies above are accompanied by or complemented with numerous theoretical works on water adsorption at Cu(110). Density-functional theory (DFT) was applied to gain insight into the adsorption structure and energetics for single monomers [20,21,17,22], dimers [21], trimers, tetramers and small clusters [23,24], chain structures [17,19] and complete monolayers [20,13,22,25,16,26].

What is missing, however, is a comprehensive study, where the water adsorption structures starting from single monomers, small clusters to one-dimensional chain structures and complete monolayers are

* Corresponding author. Tel.: +43 6803181559.
E-mail address: amirreza.baghbanpourasl@jku.at (A. Baghbanpourasl).

0039-6028/$ – see front matter © 2013 Elsevier B.V. All rights reserved.
http://dx.doi.org/10.1016/j.susc.2013.02.016

investigated on the same footing. The present work shall fill this gap. Based on DFT total-energy calculations for a large variety of structures, surface phase diagrams are calculated that give insight about the thermodynamically stable H_2O/Cu(110) surface structures. The influence of dispersion forces on the water adsorption is studied using a semi-empirical DFT-D scheme.

2. Methodology

The calculations are performed using density functional theory (DFT) within the generalized gradient approach (GGA) as implemented in the Vienna *Ab initio* Simulation Package (VASP) [27]. The electron–ion interaction is described by the projector-augmented wave scheme [28]. The electronic wave functions are expanded into plane waves up to a kinetic energy of 400 eV. Convergence tests with larger energy cutoffs show that the total adsorption energies reported here are converged within 10 meV, while the error bar for adsorption energy differences is below 5 meV. Gaussian smearing with an energy broadening of 0.2 eV is used.

The surface is modeled by periodically repeated slabs. Each supercell consists of seven Cu layers plus the adsorbed water as well as a vacuum region of about 10 Å. The uppermost four Cu layers as well as the adsorbate degrees of freedom are allowed to relax until the forces on the atoms are below 50 meV/Å. The Brillouin zone integration is performed using Monkhorst–Pack meshes with a k-point density equivalent to $8 \times 12 \times 1$ for a (1×1) surface unit cell. For the accurate calculation of chain–chain interactions we found it necessary to increase the k-point density by a factor of nine.

We use the PW91 functional [29] to describe the electron exchange and correlation energy within the GGA. It describes the hydrogen bonds in solid water (ice Ih) in good agreement with experiment [30,31].

The accurate modeling of loosely bonded adsorbates is a major challenge for density-functional theory (DFT), because the currently used XC energy functionals do not properly describe the long-range van der Waals (vdW) interactions [32–37]. The importance of vdW forces for surface wetting properties was recently pointed out by Michaelides and co-workers [38]. In order to account approximately for dispersion interactions, we use a semi-empirical, so-called DFT-D scheme [39,40] based on the London dispersion formula. Reuter and co-workers [35] compared molecular adsorption energies calculated within various DFT-D schemes for coinage metal surfaces with experiment and concluded that the approach by Ortmann et al. [39,40] – the one which is used in the following – provides results in the "*right ballpark and could even be semiquantitative*". It should be kept in mind, however, that the accurate description of dispersion forces for complex systems still is a somewhat open problem [36]. Even more realistic and numerically far more involved approaches than DFT-D, such as the vdW density-functional (vdW-DF) method [41] do not necessarily lead to an accurate description of adsorption phenomena [37]. In this sense the present DFT-D results should be cautiously interpreted as indications for the trend that can be expected from the inclusion of vdW effects.

The present Cu(110) surface calculations were performed using the equilibrium lattice constants of 3.634 and 3.599 Å calculated within DFT–GGA and DFT-D, respectively. The experimental value at room temperature amounts to 3.615 Å. The calculations of the clean Cu(110) surface yield a shrinking of the distance between the first and the second layer of −9.5% (DFT-D: −7.6%) and an increase in distance of 3.9% (DFT-D: 4.1%) between the second and third layer. This agrees with the experimental observations, see, *e.g.*, Refs. [42,43].

The adsorption energy calculated here refers to the difference in energy (per adsorbed molecule) between the relaxed adsorbed geometry and the clean Cu(110) surface plus the energy of the respective water molecules calculated in gas phase. In the case of structures containing hydroxyl groups it is assumed that the dissociated hydrogen atoms bond separately on the bare copper surface and energy of this bonding is considered in calculation of adsorption energy. In order to compare energetically adsorption models with different coverages, the thermodynamic grand canonical potential

$$\begin{aligned}\Omega\left(\mu^{H_2O}\right) &= F_{surf}(n_i) - n_{H_2O}\mu^{H_2O} \\ &\approx E_{surf}(n_i) - n_{H_2O}\mu^{H_2O}\end{aligned}$$

needs to be calculated [44], where $F_{surf}(n_i)$ is the surface free energy which we approximate by the total surface energy $E_{surf}(n_i)$ at zero temperature and n_{H_2O} is the total number of adsorbed water molecules. Given that the adsorption energies calculated here are far larger than the typical electronic or vibrational contributions to the free energy [45,46], this approximation seems justified. In fact, our calculations indicate an error bar of about 15 meV per molecule in energy difference between the structures to result from the neglect of the molecular vibrations at 500 K. Also the neglect of the zero point energies (see, *e.g.*, Ref. [47]) does not affect the relative stabilities of surface energies or the calculated phase diagrams noticeably. The grand canonical potential can be conveniently related to the adsorption energy E_{ads} by

$$\Omega\left(\mu^{H_2O}\right) = \left(E^{H_2O@gas} - \mu^{H_2O} - E^{ads}\right)\theta$$

where $E^{H_2O@gas}$ is the total energy of a water molecule in gas phase and θ is the coverage.

In the calculated phase diagrams Ω *vs.* μ_{H_2O} the water chemical potential is given with respect to the calculated energy of molecular water at zero temperature. In order to relate the calculated surface energies to experimental observables such as pressure and temperature, we also calculate the change of the water chemical potential using the approximation of a polyatomic ideal gas [48]

$$\Delta\mu_{H_2O}(p,T) = k_B T\left[\ln\left(\frac{p\lambda^3}{k_B T}\right) - (\ln)(Z_{rot}) - ln(Z_{vib})\right].$$

Here k_B is the Boltzmann constant, T is the temperature, p is the pressure, $\lambda = \sqrt{h^2/2m\pi k_B T}$ is the de Broglie thermal wave length, and

$$Z_{rot} = \frac{\sqrt{\pi I_1 I_2 I_3}(2k_B T)^{3/2}}{\sigma\hbar^3},$$

and

$$Z_{vib} = \prod_{\alpha}\left[1 - exp\left(-\frac{\hbar\omega_\alpha}{k_B T}\right)\right]^{-1}$$

are the rotational and vibrational partition functions, respectively. The calculated values for the water chemical potential agree well with the data in JANAF database [49] for the respective pressures and temperatures.

3. Results and discussion

The experimentally observed water overlayer structures can be categorized into (a) single monomers or small clusters consisting of a few molecules and (b) extended, periodic structures such as one-dimensional chains or two-dimensional overlayers.

We first optimized the atomic geometries of small clusters consisting of up to five water molecules, considering adsorption structures suggested earlier [22,24]. The energetically most relevant structures are shown in Fig. 1. In all cases, a number of plausible starting configurations with adsorption in on-top, hollow, long-bridge or short-bridge sites was probed and structurally relaxed. In case of the monomer,

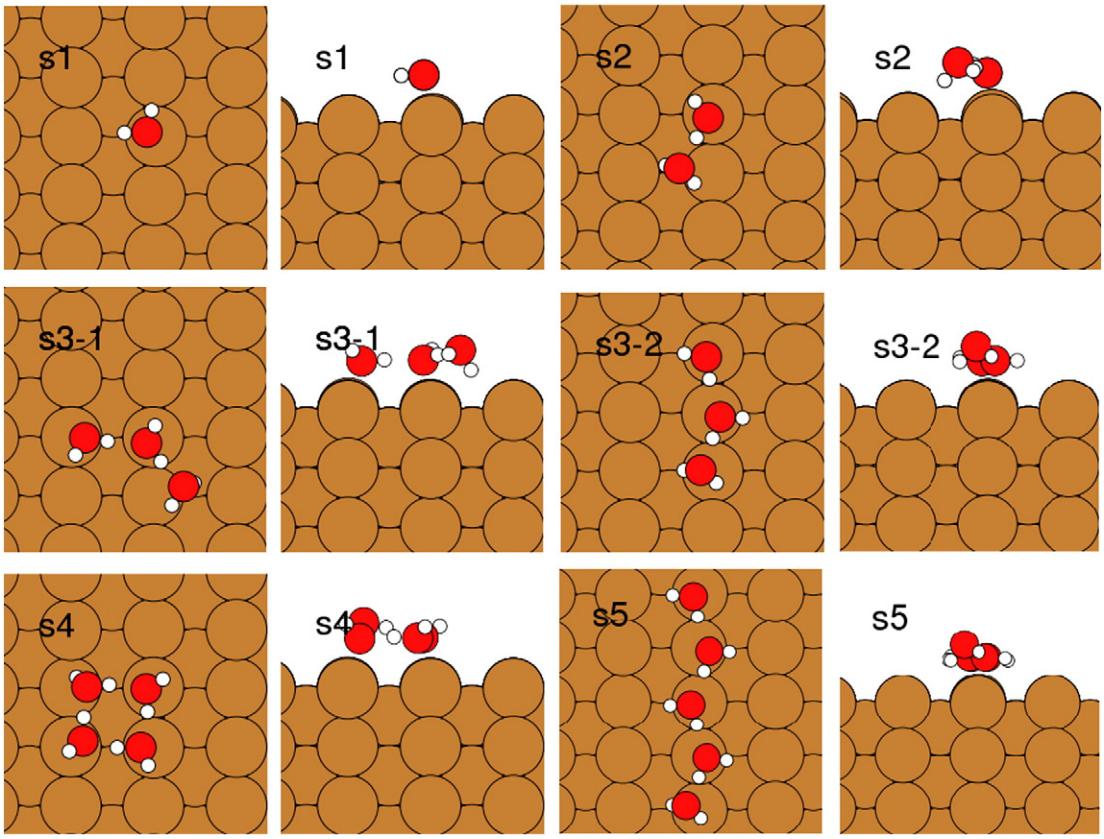

Fig. 1. Schematic top and side views of energetically favorable monomer and cluster adsorption geometries. Large, medium, and small circles represent copper, oxygen, and hydrogen atoms.

the energetically most favorable geometry yields a DFT adsorption energy of 0.357 eV (*cf.* compilation of values in Table 1). Including vdW interactions considerably increases the adsorption energy to 0.585 eV. In both cases the most stable geometry is placed in on-top position, but within DFT-D the molecule faces the hollow rather than the long-bridge site.

Increasing the cluster size initially enhances the adsorption energy per water molecule, as shown in Fig. 2, since the additional hydrogen bonds between the water molecules stabilize the adsorption configuration. We find this increase to saturate by increasing the size of the chain. In fact the most stable cluster consisting of four molecules found here has a slightly higher adsorption energy per atom than the pentamer, because a cyclic tetramer is commensurable with favorable substrate bonding positions, thus it constitutes an extra hydrogen bond which leads to higher adsorption energy. It is interesting to note that the energetic preference for tetramers does not depend on the use of DFT or DFT-D. This agrees with the findings by Carrasco et al. [38], who concluded that "*while dispersion is important for the absolute adsorption energy of water it is of less importance to the atomic structure*". The comparison of s3-1 and s3-2 shows the interplay between water–water hydrogen bonds and favorable adsorption sites: Water prefers to form ice-like structures which favors the bent structure. On the other hand, however, the on-top sites on Cu are the preferred adsorption sites. The trade off yields in our calculations a

Table 1
Calculated adsorption energies in eV (within DFT and DFT-D) for the energetically most relevant geometries per water/hydroxyl molecule. The adsorption energies for non-stoichiometric structures are calculated assuming that the hydrogen atoms adsorb on Cu(110) (desorb as H_2).

Structure	E_{ads}^{DFT-D}	E_{ads}^{DFT}	Previous DFT
s1 (monomer)	0.585	0.357	0.375 [22]
s2 (dimer)	0.753	0.431	–
s3-1 (trimer) (bent)	0.827	0.495	0.457 [24]
s3-2 (trimer) $[1\bar{1}0]$	0.819	0.486	0.458 [24]
s4 (tetramer)	0.885	0.519	0.504 [24]
s5 (pentamer)	0.838	0.509	–
m1 (H-down)	1.001	0.559	0.554 [22]
m2 (H-up)	0.867	0.526	0.514 [22]
m3 (chain-like)	0.989	0.564	0.560 [22]
m4 (H-up-down)	0.956	0.561	–
d1	0.789	0.468	0.632 [22]
d2	0.894 (0.770)	0.602 (0.542)	0.655 [16]
d3	0.999 (0.916)	0.658 (0.618)	0.700 [16]
c1 (pentagonal chain)	0.955	0.590	0.59 [19]
c2 (mixed H_2O and OH)	0.878 (0.795)	0.591 (0.552)	–
c3 (pure OH)	0.560 (0.312)	0.398 (0.279)	–

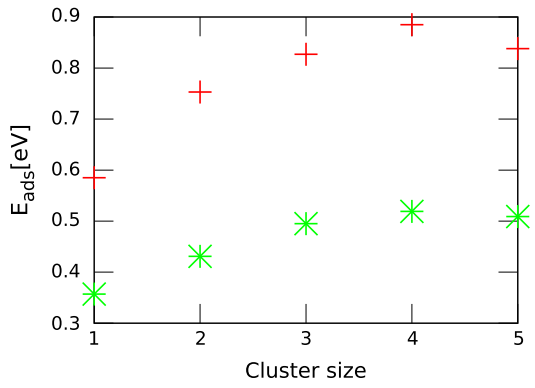

Fig. 2. Calculated DFT-D (crosses) and DFT (stars) adsorption E_{ads} for the enegetically most favored cluster geometries consisting of up to five molecules.

slightly (~1–2%) higher adsorption energy for the bent structure. Again, this result does not depend on the use of DFT or DFT-D.

In order to model the experimentally observed chain structures, we study the structures shown schematically in Fig. 3. Thereby c1 is a chain of water molecules arranged in pentagons along the [001] direction. Structures c2 and c3 are parallel to the $[1\bar{1}0]$ direction. Structure c2 consists of H_2O and OH in the ratio of 2:1 and c3 consists of hydroxyl groups only. The c1 pentagon structure has been proposed in Ref. [19]. In order to probe possible chain–chain interactions we performed calculations for a variety of c1–c1 chain distances. It is found that the DFT adsorption energy increases by increasing the distance (d) between the chains, *i.e.*, there is a repulsive interaction between the chains. As shown in Fig. 4, the chain–chain interaction within DFT scales approximately with $1/d$ (with only minor modifications within DFT-D), indicating an electrostatic charge–charge repulsion with little influence of substrate screening.

Although the energy modification due to the long-range repulsion is clearly very small and approaches the numerical and methodological accuracy of our calculations, the trend found here may explain the self-assembly of equally spaced parallel chains as observed experimentally [18,17,19]. The $1/d$ scaling of the chain–chain interaction energy is modified for smaller distances in case of DFT-D calculations. In fact, in case of the c3 structure seemingly an attraction between the rows is caused by the vdW interaction. However, the energy differences are so small that this finding may as well be related to numerical artifacts.

In order to analyze the interaction between c1 chains in more detail, we study the electron redistribution due to the formation of this structure, see Fig. 5. It was calculated by subtracting from the electron density of the structure with water adsorbed, the sum of the electron charges of the bare surface and the water molecules at the same positions, non-interacting with the surface. The laterally integrated electron density shown (rhs) indicates charge accumulation between the top surface Cu atoms and hydrogen atoms that are closest to the surface. The bottom panel in Fig. 5 shows the electron density redistribution in the plane parallel to the surface passing between surface atoms and adsorbate. Obviously, the above mentioned electron accumulation occurs mainly below the vertically standing water molecules. From the left panel in this figure it is clear that the electron accumulation underneath the water molecule does not cause a microscopic image charge in the metal, in contrast to heuristic arguments from macroscopic electrostatics sometimes found in literature.

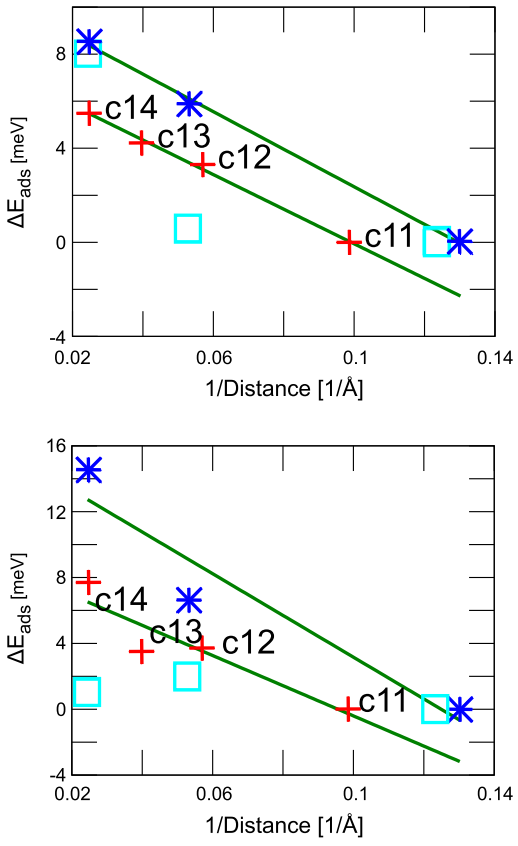

Fig. 4. Calculated adsorption energy differences for various chain structures *vs.* the closest O–O distance between the chains. DFT and DFT-D results are shown in the upper and lower panel, respectively. Crosses, stars, and squares denote c1, c2, and c3 chain structures. The calculations were done with k-point meshes equivalent to $24 \times 36 \times 1$ for the 1×1 surface unit cell.

This may explain the point charge-like repulsion ($\propto r^{-1}$) between neighboring chains. It is further seen (right panel of Fig. 5) that the adsorption induced electron density redistribution in the metal decays fast. Already in the third layer it is reduced to about 10% of the surface value. However, it should be kept in mind that the chain–chain interactions may also be affected by Friedel oscillations of the substrate

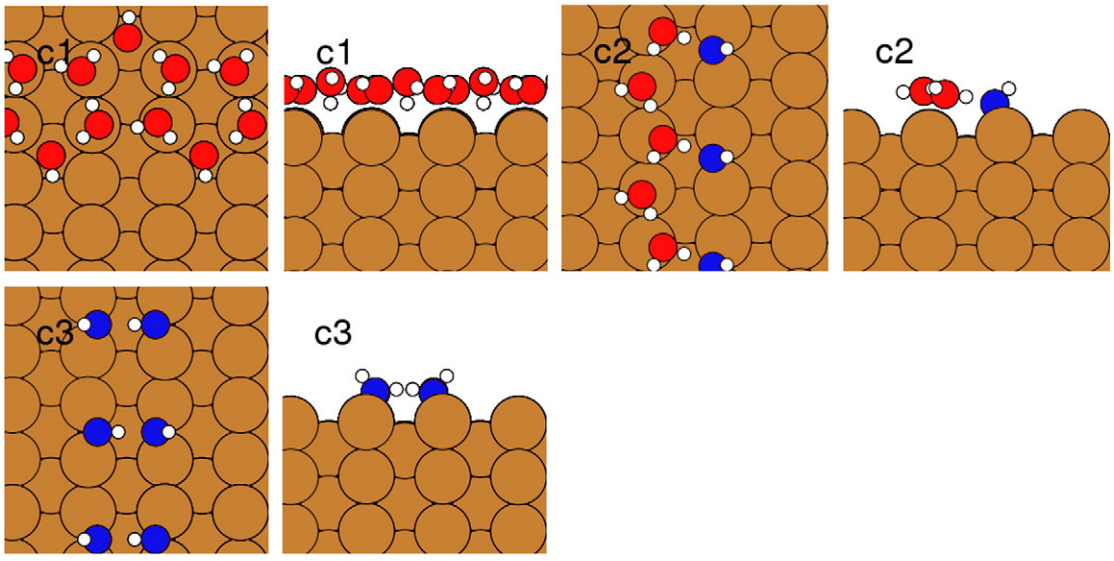

Fig. 3. One dimensional chain structures. Oxygen atoms in water and hydroxyl groups are shaded differently.

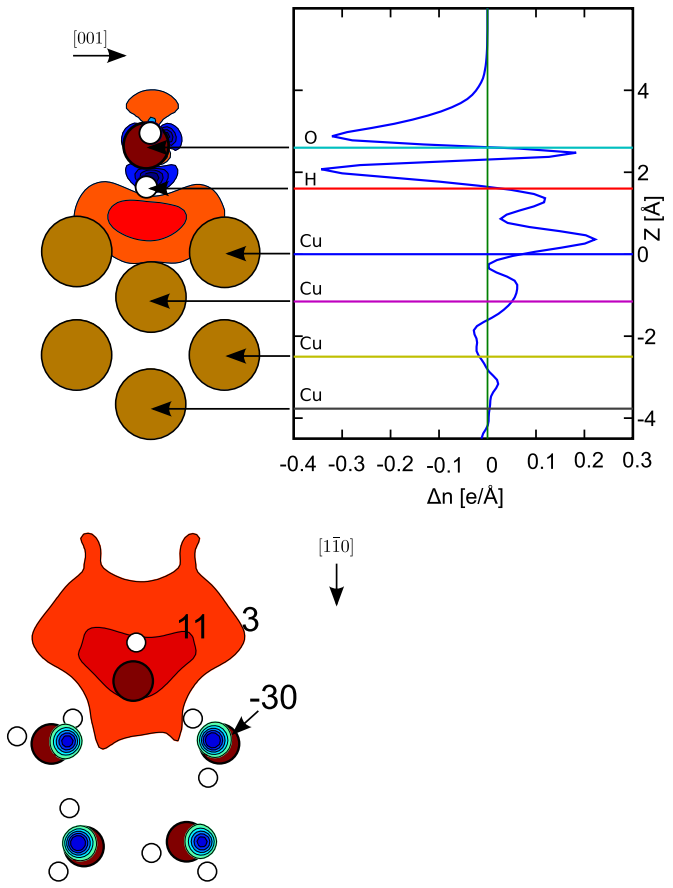

Fig. 5. Electron density redistribution due to water c1 chain adsorption. Left: Contour map (isolines in units of 0.001 e/Å^3) in the plane $(1\bar{1}0)$, passing through the vertically standing water molecule. Four copper layers are shown. Right: Laterally averaged density redistribution *vs.* the surface normal. The coordinates of Cu, H and O atoms are indicated. Bottom: Contour map in a plane parallel to the surface, passing between surface Cu atoms and adsorbate.

electrons [50,51] as well as by adsorption-induced strain fields in the substrate [52].

Experimentally, also water-hydroxyl chains were observed in low temperature experiments [17]. Here this structure is modeled with the c2 geometry shown in Fig. 3. The chain forms along the $[1\bar{1}0]$ direction and consists in each unit cell of two water molecules which constitute the backbone of the chain and are connected by a hydrogen bond and a hydroxyl group. This chain also interacts repulsively (stars in Fig. 4) with its neighbor chains; the repulsive interaction causes again the appearance of a self ordered parallel chain structure as observed in the experiment [17]. Structures like c3, suggested in Ref. [17], consist of a sequence of two OH molecules (Fig. 3) that are assumed to form a stable configuration. In the chain structures c1 and c2 hydrogen bonds interlock the building blocks (water and hydroxyl) of the chain and keep its integrity. In contrast, the c3 chain is different in the sense that it does not form bonds between the constituting $(OH)_2$ units. Consequently, the present DFT and DFT-D simulations (performed with the same high density k-point mesh used above to calculate the chain interactions) show that stretching the chain even by a factor of three does not reduce the adsorption energy. From this result we conclude that the c3 structure proposed in Ref. [17] is not likely to describe stable OH group chains.

Finally, we consider structures derived from hexagonal ice Ih-like bonding configurations that correspond to monolayer coverage within a c(2 × 2) translational symmetry [8,9,13,22,16]. At low temperature water adsorbs on the clean Cu(110) surface and does not dissociate owing to the high activation energy for dissociation of water molecules [22]. This overlayer consists of two sublayers, in the one closer to the surface water molecules (*i.e.* their bonds) are parallel to surface (Fig. 6). Water molecules in the second layer can be oriented differently. Depending on the direction of the non-hydrogen bonded OH they are either called H-down or H-up (m1/m2 in Fig. 6). Chain-like configurations such as m3 are also conceivable. Water molecules on close packed surfaces like Pt(111) adsorb in H-down configuration [53]. On the open surface of Cu(110) a mixture of H-down and H-up is observed experimentally [13]. The DFT results in Table 1 are in agreement with the observation, that despite the pure H-down configuration is more stable than the pure H-up, their mixture (m4) makes the structure even more stable, most likely due to the optimized dipole–dipole interaction. Given the large number of possibilities to arrange patterns of H-up and H-down molecules, structures that are energetically even more favorable than the one found here cannot be excluded. Moreover, the precise energetic ordering of the monolayer structures is sensitive with respect to the usage of DFT or DFT-D: Within the latter, the pure H-down structure is the most stable structure. Obviously, dispersion interactions may be decisive for the adsorption geometry in case of energetically nearly degenerate structures.

Experimentally, on oxygen preadsorbed Cu(110) surfaces, or after electron bombardment of the water covered surface, adsorption structures containing hydroxyl groups are observed [14,16]. Previously suggested structural models for this overlayer containing both water molecules and OH groups are shown in Fig. 7. The d1 [22] and d2 structures [16] have a (2 × 2) unit cell and contain equal amounts of H_2O and OH. In case of the Ru(0001) surface, d1-type structures were found to be more stable than hexagonal water structures [5]. The present calculations – irrespective of whether or not vdW is included – find the partially dissociated d1 structure to be less stable than the intact H-down structure on Cu(110), in deviation to the findings of Ren and Meng [20,22]. This may be a result of the finer and more isotropic k-point sampling in the present work. The structure d3 contains two Bjerrum defects per (2 × 6) unit cell (dashed black rectangle in the bottom panel of Fig. 7), for each defect two H atoms face each other, not contributing to hydrogen bonding. This structure has been experimentally observed [16] on oxygen precovered surfaces at $T \leq 140$ *K* in ultra high vacuum STM and under electron exposure [13,16,11]. It contains H_2O and OH groups with a ratio of 2:1 and is energetically most favored among the OH containing structures considered in the present work, both within DFT and DFT-D. The calculations show that the lower coordination of some oxygen atoms in the d3 structure leads to stronger hydrogen bonds; they are about 0.1 Å shorter than in d2.

The construction of surface phase diagrams based on calculations of the grand-canonical potential provides a consistent way of energetically comparing surfaces with different coverages and stoichiometries. This approach has been applied already to a variety of water–solid interfaces, see Refs. [54,55]. The calculated phase diagrams show which structures (and under which experimental conditions) are thermodynamically stable and may be observed. Fig. 8 shows phase diagrams calculated within DFT (a and b) and DFT-D (c and d). Thereby the Fig. 8a contains all energetically relevant adstructures considered in our study, and Fig. 8b is restricted to molecular adsorption and does not consider structures that contain additional OH groups which can be created due to adsorption of water on oxygen preadsorbed surfaces, electron bombardment or partial thermal dissociation at temperatures above 150 K [11]. Among all adstructures considered in the present work, the d3 structure containing hydroxyl groups and Bjerrum defects is the most stable. At increasingly drier conditions, *i.e.*, for lower values of μ^{H_2O}, the clean surface is favored. For ultra high vacuum conditions ($\approx 10^{-7}$ Pa), the water desorption will occur at temperature 175 K, according to the DFT calculations. This agrees with temperature programmed desorption (TPD) experiment showing water desorption peak at 185 K [26]. In the absence of preadsorbed oxygen, water desorption occurs at 160 K which is in

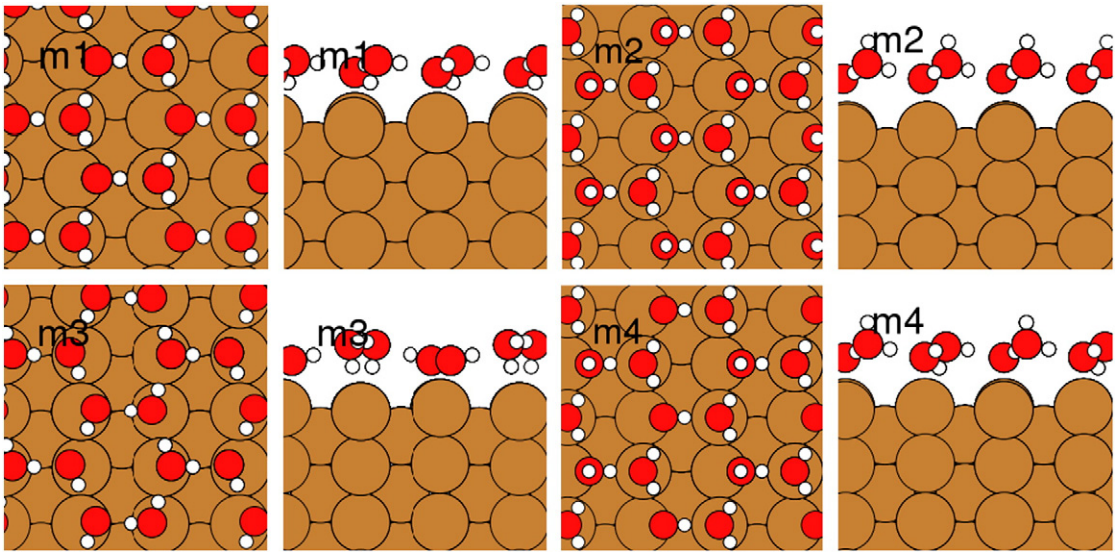

Fig. 6. Models for complete monolayers formed by water molecules within a c(2 × 2) translational symmetry.

accordance with TPD peak at 165 K [17,26]. These results are depicted in Fig. 9. In this case DFT also predicts a narrow range of preparation conditions where between the water monolayer-covered (m1 represents here the family of energetically nearly degenerate water monolayer structures) and the bare surface, pentagon chains (c1 structure) will be stable. As shown in Fig. 4, the chain adsorption energy depends on the chain distance. Accordingly, different chain structures become stable for different values of the water chemical potential, giving rise to a continuous phase change. This is demonstrated in the small inset of Fig. 8b. The calculations thus predict a smooth change from the bare surface, to a water-chain covered surface with decreasing chain distance to the formation of a closed two-dimensional overlayer. This agrees with the experimental observation [19] of a decreased chain distance upon increasing the water dosage. From the many adstructures considered here, only few correspond to thermodynamically stable structures: a hexagonal network of water-hydroxyl trimers containing Bjerrum defects (d3), ice-like water monolayer (m1) and water chains consisting of pentagons (c1). Of course, this does not necessarily mean that no other structures will occur. Obviously also kinetics dictates the water film morphology, in particular in low-temperature and low-pressure experiments, where structures such as c2 chains or water clusters have been experimentally prepared (*e.g.* clusters assembled by STM in Ref. [24]).

The influence of the vdW interactions on the surface phase diagram is shown in Fig. 8c and d, which contains the present DFT-D results. Mainly the transition temperature between water-covered and bare surfaces is increased due to the dispersion forces. We find a shift between about 60 K for low pressures and 150 K at near ambient pressures. Comparing the calculated data to the experiment, the DFT-D results seem closer to the measured findings at higher temperatures (Fig. 9). For example in Ref. [12] large quantities of molecular water on the surface were observed up to 428 K in 1 Torr. On the other

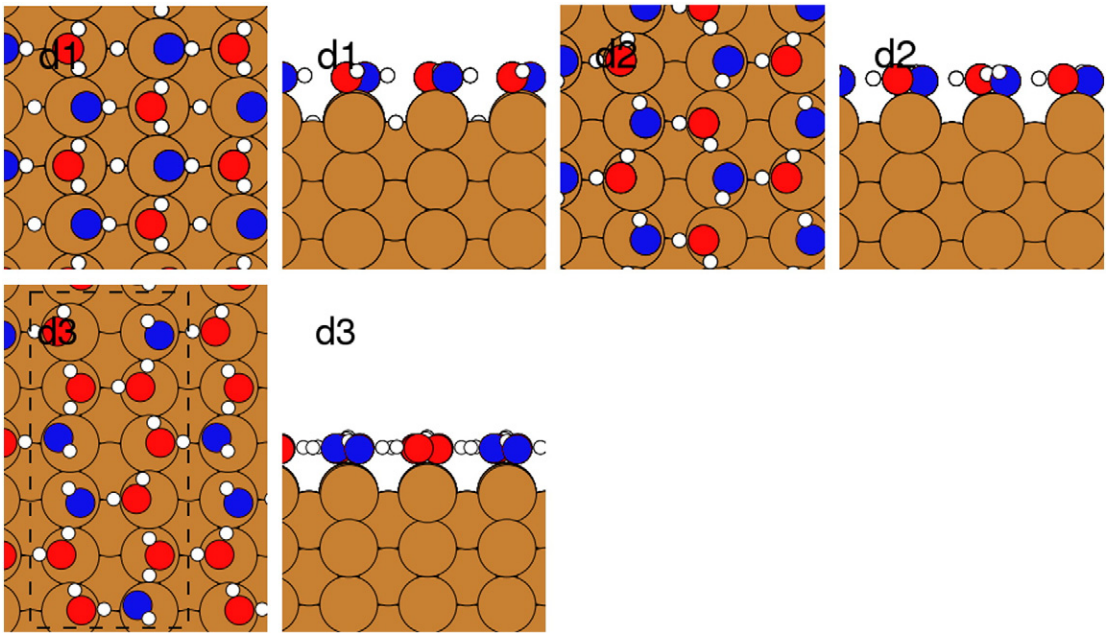

Fig. 7. Extended overlayer structures containing hydroxyl groups in addition to water Bjerrum defect is modeled with d3. Oxygen atoms in water and hydroxyl groups shaded differently.

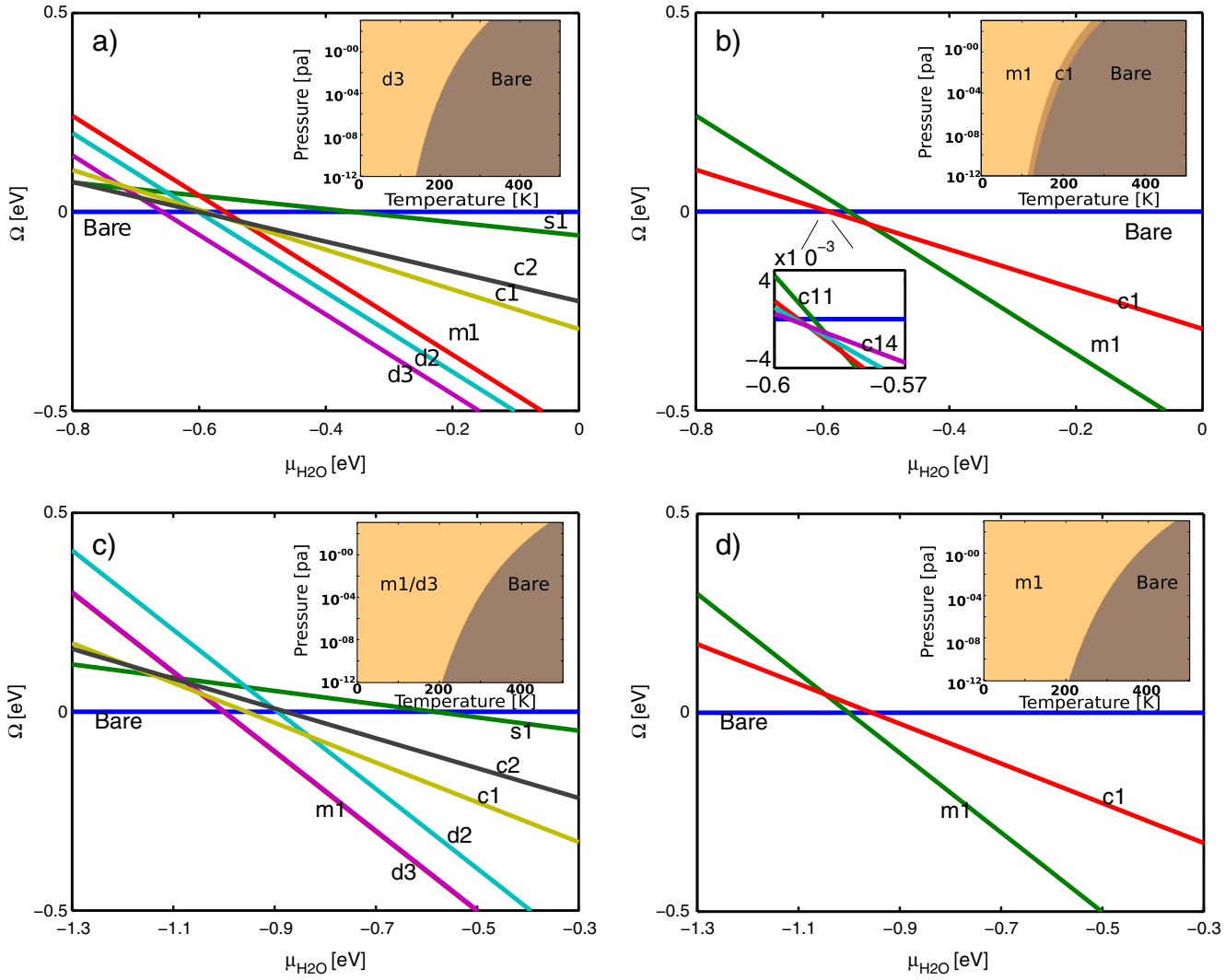

Fig. 8. Calculated phase diagrams of the Cu(110) surface. (a) and (b) are DFT and (c) and (d) are DFT-D calculations. The rhs plots (b) and (d) restrict the energetic comparison to structures where only water molecules and no separate hydroxyl groups are present on the surface.

hand, due to slight changes of the relative adsorption energies, the (experimentally observed) c1 chain does not occur in the phase diagram anymore. It is now less favored than the m1 monolayer. This is not necessarily an indication that this structure is only kinetically stabilized, but may be an artifact of the specific DFT-D implementation used here. We mention that Carrasco et al. [38], using a modified version of vdW-DF, found no reversal of the energy ordering between c1 and the monolayer structures due to dispersion forces. As stressed in Ref. [38] "*we are still some way from quantitative first principles predictions of wetting and related phenomena*". Possibly only numerically very involved schemes like the random phase approximation within the adiabatic connection fluctuation dissipation theorem will provide a definite answer to energetic subtleties such as the stability range of the c1.

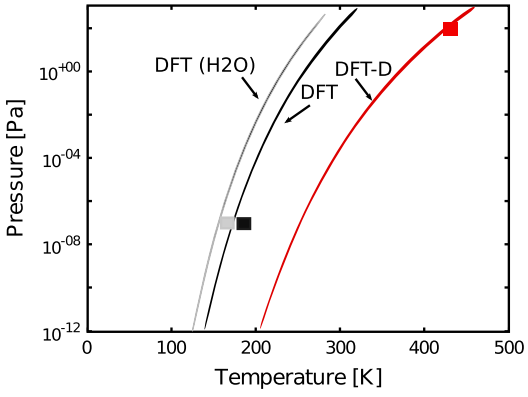

Fig. 9. Water desorption temperature for any given pressure calculated with DFT and DFT-D. Squares show the experimental values from Refs. [17,26]. The left line corresponds to the desorption temperature in the absence of preadsorbed oxygen.

4. Conclusion

DFT and DFT-D calculations for ultrathin water films and water clusters adsorbed on the Cu(110) surface were performed. Surface phase diagrams were calculated that allow for a consistent energetic comparison of the many structures proposed previously for this system. Starting from single admolecules, the adsorption energy is found to increase with increasing cluster size up to four molecules forming tetramers. Although the adsorption energy increases considerably (by more than 0.2 eV) upon including van der Waals interactions, the relative energetic order of the cluster geometries is relatively robust with respect to the use of DFT or DFT-D for the calculations. The comparison of the cluster adsorption energies with either complete ice-like water monolayers or Bjerrum-defect stabilized water-hydroxyl group

layers shows that the former are unstable with respect to coalescence, irrespective of whether or not vdW forces are included. In addition to the completely water covered surface, however, an additional phase is found to be thermodynamically stable. It consists of parallel chains formed by water pentagons. These chains interact repulsively due to Coulomb forces and are thus expected to self-assemble with equal distances. The chain–chain distances decrease with increasing water dosage in such a way to realize a gradual transition between the bare and the completely water-covered surface. The various monolayer structures considered here as well as the pentagon chain structure are close in energy. Dispersion forces increase the calculated desorption temperatures by about 60 (at lower pressures) to 150 K (at higher pressures), which in near ambient conditions is in very good agreement with experiments that are expected to be close to thermodynamic equilibrium.

Acknowledgments

The authors thank Peter Zeppenfeld and Norbert Esser for very helpful discussions and valuable comments on the manuscript. Grants of computing time from the Johannes Kepler University of Linz and technical support of Johann Messner is gratefully acknowledged. We thank the Wilhelm Macke Foundation and the Deutsche Forschungsgemeinschaft for financial support.

References

[1] M. Henderson, Surf. Sci. Rep. 46 (2002) 1.
[2] A. Hodgson, S. Haq, Surf. Sci. Rep. 64 (9) (2009) 381.
[3] P. Wernet, D. Nordlund, U. Bergmann, M. Cavalleri, M. Odelius, H. Ogasawara, L.Å. Naäslund, T.K. Hirsch, L. Ojamäe, P. Glatzel, L.G.M. Pettersson, A. Nilsson, Science 304 (2004) 995.
[4] A. Hermann, W.G. Schmidt, P. Schwerdtfeger, Phys. Rev. Lett. 100 (2008) 207403.
[5] P.J. Feibelman, Science 295 (2002) 99.
[6] P.J. Feibelman, Phys. Rev. Lett. 90 (2003) 186103.
[7] A. Michaelides, K. Morgenstern, Nat. Mater. 6 (2007) 597.
[8] A. Spitzer, H. Lüth, Surf. Sci. 120 (1982) 376.
[9] C. Mariani, K. Horn, Surf. Sci. 126 (1983) 279.
[10] C. Ammon, A. Bayer, H.P. Steinrück, G. Held, Chem. Phys. Lett. 377 (2003) 163.
[11] K. Andersson, A. Gomez, C. Glover, D. Nordlund, H. Ostrom, T. Schiros, O. Takahashi, H. Ogasawara, L. Pettersson, A. Nilsson, Surf. Sci. 585 (3) (2005) L183.
[12] K. Andersson, G. Ketteler, H. Bluhm, S. Yamamoto, H. Ogasawara, L.G.M. Pettersson, M. Salmeron, A. Nilsson, J. Phys. Chem. C 111 (2007) 14493.
[13] T. Schiros, S. Haq, H. Ogasawara, O. Takahashi, H. Ostrom, K. Andersson, L.G.M. Pettersson, A. Hodgson, A. Nilsson, Chem. Phys. Lett. 429 (4) (2006) 415.
[14] S. Yamamoto, K. Andersson, H. Bluhm, G. Ketteler, D.E. Starr, T. Schiros, H. Ogasawara, L.G.M. Pettersson, M. Salmeron, A. Nilsson, J. Phys. Chem. C 111 (22) (2007) 7848.
[15] K. Andersson, G. Ketteler, H. Bluhm, S. Yamamoto, H. Ogasawara, L.G.M. Pettersson, M. Salmeron, A. Nilsson, J. Am. Chem. Soc. 130 (2008) 2793.
[16] M. Forster, R. Raval, A. Hodgson, J. Carrasco, A. Michaelides, Phys. Rev. Lett. 106 (2011) 046103.
[17] J. Lee, D.C. Sorescu, K.D. Jordan, J.T. Yates, J. Phys. Chem. C 112 (45) (2008) 17672.
[18] T. Yamada, S. Tamamori, H. Okuyama, T. Aruga, Phys. Rev. Lett. 96 (2006) 036105.
[19] J. Carrasco, A. Michaelides, M. Forster, S. Haq, R. Raval, A. Hodgson, Nat. Mater. 8 (5) (2009) 427.
[20] J. Ren, S. Meng, J. Am. Chem. Soc. 128 (2006) 9282.
[21] Q.-L. Tang, Z.-X. Chen, J. Chem. Phys. 127 (2007) 104707.
[22] J. Ren, S. Meng, Phys. Rev. B 77 (5) (2008) 054110.
[23] T. Kumagai, M. Kaizu, H. Okuyama, S. Hatta, T. Aruga, I. Hamada, Y. Morikawa, Phys. Rev. B 81 (4) (2010) 045402.
[24] T. Kumagai, H. Okuyama, S. Hatta, T. Aruga, I. Hamada, J. Chem. Phys. 134 (2) (2011) 024703.
[25] T. Schiros, H. Ogasawara, L.A. Näslund, K.J. Andersson, J. Ren, S. Meng, G.S. Karlberg, M. Odelius, A. Nilsson, L.G.M. Pettersson, J. Phys. Chem. C 114 (2010) 10240.
[26] M. Forster, R. Raval, J. Carrasco, A. Michaelides, A. Hodgson, Chem. Sci. 3 (1) (2012) 93, http://dx.doi.org/10.1039/c1sc00355k, (URL http://xlink.rsc.org/?DOI=c1sc00355k).
[27] G. Kresse, J. Furthmüller, Comput. Mater. Sci. 6 (1996) 15.
[28] G. Kresse, D. Joubert, Phys. Rev. B 59 (1999) 1758.
[29] J.P. Perdew, J.A. Chevary, S.H. Vosko, K.A. Jackson, M.R. Pederson, D.J. Singh, C. Fiolhais, Phys. Rev. B 46 (1992) 6671.
[30] D.R. Hamann, Phys. Rev. B 55 (1997) R10157.
[31] C. Thierfelder, A. Hermann, P. Schwerdtfeger, W.G. Schmidt, Phys. Rev. B 74 (2006) 045422.
[32] W.G. Schmidt, K. Seino, M. Preuss, A. Hermann, F. Ortmann, F. Bechstedt, Appl. Phys. A 85 (2006) 387.
[33] M. Rohlfing, T. Bredow, Phys. Rev. Lett. 101 (26) (2008) 266106, http://dx.doi.org/10.1103/PhysRevLett.101.266106.
[34] N. Atodiresei, V. Caciuc, P. Lazić, S. Blügel, Phys. Rev. Lett. 102 (13) (2009) 136809, http://dx.doi.org/10.1103/PhysRevLett.102.136809.
[35] E.R. Mcnellis, J. Meyer, K. Reuter, Phys Rev B 80 (2009) 205414.
[36] G. Mercurio, E.R. McNellis, I. Martin, S. Hagen, F. Leyssner, S. Soubatch, J. Meyer, M. Wolf, P. Tegeder, F.S. Tautz, K. Reuter, Phys. Rev. Lett. 104 (3) (2010) 036102, http://dx.doi.org/10.1103/PhysRevLett.104.036102.
[37] C. Thierfelder, M. Witte, S. Blankenburg, E. Rauls, W. Schmidt, Surf. Sci. 605 (2011) 746.
[38] J. Carrasco, B. Santra, J. Klimeš, A. Michaelides, Phys. Rev. Lett. 106 (2) (2011) 026101.
[39] F. Ortmann, W.G. Schmidt, F. Bechstedt, Phys. Rev. Lett. 95 (2005) 186101.
[40] F. Ortmann, F. Bechstedt, W.G. Schmidt, Phys. Rev. B 73 (2006) 205101.
[41] M. Dion, H. Rydberg, E. Schröder, D.C. Langreth, B.I. Lundqvist, Phys. Rev. Lett. 92 (2004) 246401.
[42] D.L. Adams, H.B. Nielsen, J.N. Andersen, I. Stensgaard, R. Feidenhans, l J.E. Sørensen, Phys. Rev. Lett. 49 (1982) 669.
[43] J.L.F. Da Silva, K. Schroeder, S. Blügel, Phys. Rev. B 69 (24) (2004) 245411.
[44] G.-X. Qian, R.M. Martin, D.J. Chadi, Phys. Rev. Lett. 60 (1988) 1962.
[45] M. Valtiner, M. Todorova, G. Grundmeier, J. Neugebauer, Phys. Rev. Lett. 103 (6) (2009) 065502, http://dx.doi.org/10.1103/PhysRevLett.103.065502.
[46] S. Wippermann, W.G. Schmidt, Phys. Rev. Lett. 105 (2010) 126102.
[47] D. Donadio, L.M. Ghiringhelli, L. Delle Site, J. Am. Chem. Soc. 134 (46) (2012) 19217.
[48] L.D. Landau, E.M. Lifshitz, Statistical Physics, Part I, 3rd edition Butterworth Heinemann, Oxford, 1981.
[49] M.W. Chase, C.A. Daives, J.R. Downey, D.J. Frurip, R.A. McDonald, A.N. Syverud, J. Phys. Chem. Ref. Data 14 (1985) 1.
[50] K.H. Lau, W. Kohn, Surf. Sci. 75 (1978) 69.
[51] S. Blankenburg, W.G. Schmidt, Phys. Rev. B. 78 (2008) 233411.
[52] S. Blankenburg, W.G. Schmidt, Phys. Condens. Matter 21 (2009) 185001.
[53] H. Ogasawara, B. Brena, D. Nordlund, M. Nyberg, A. Pelmenschikov, L.G.M. Pettersson, A. Nilsson, Phys. Rev. Lett. 89 (2002) 276102.
[54] P. Thissen, G. Grundmeier, S. Wippermann, W.G. Schmidt, Phys. Rev. B 80 (2009) 245403.
[55] C. Thierfelder, W.G. Schmidt, Phys. Rev. B 82 (2010) 115402.